ARCHIVES
of
FOUNDRY ENGINEERING

ISSN (2299-2944)
Volume 2026
Issue 2/2026

49 – 62

10.24425/afe.2026.157989

6/2

Published quarterly as the organ of the Foundry Commission of the Polish Academy of Sciences

The Influence of Foundry Sand Type on the Hardening Process of Self-Setting Molding Sands Based on Urea-Furan Binder

N. Matonis [a] *, D. M. Halejcio [a], G. Golęba [b]

[a] AGH University of Krakow, Faculty of Foundry Engineering, Department of Moulding Materials, Mould Technology and Non-ferrous Metals
al. A. Mickiewicza 30, 30-059 Krakow, Poland

[b] AGH University of Krakow, Faculty of Materials Science and Ceramics, Department of Glass Technology and Amorphous Coatings, al. A. Mickiewicza 30, 30-059 Krakow, Poland

* Corresponding author: E-mail address: nataliamatonis@gmail.com

Received 19.12.2025; accepted in revised form 02.04.2026; available online 26.06.2026

Abstract

The article presents the results of investigations on the influence of the type of sand matrix on the binding process of self-setting molding sands with an organic binder. The study encompassed molding sands prepared on matrices of quartz, reclaimed quartz, zircon, chromite, corundum, synthetic, and olivine sand (a "non-compatible" sand). For the preparation of the molding sands, a urea–furan resin Kalthartz U404 was used as the binder, along with an acidic hardener, Activator 100 T3. In the case of matrices compatible with the self-setting molding sand system with an organic binder, the resin content was 1.00 p.p.w., with a constant hardener-to-binder ratio of 50 %. During the study, a sieve analysis of the investigated sand matrices was conducted according to PN-83/H-11076, and the pH value was determined using a method refined by the authors based on BN-81/4021-02. Fourier Transform Infrared (FTIR) spectroscopy was performed, along with kinetic studies of the sand binding process using the ultrasonic method, complemented by observations of the resulting binder bridges. During the ultrasonic tests, the influence of the applied sand matrix on the value of the obtained wave velocities (C_L) and on the changes in the degree of sand hardening (S_x) during binding was determined. Additionally, the kinetics of the hardening process were determined based on dC_L/dt and dSx/dt. All experiments were conducted on an ultrasonic testing station equipped with a temperature-controlled chamber, maintaining an ambient temperature of 20 °C throughout the measurements. Care was taken to ensure that the temperature of the molding sand after mixing all components remained at approximately 20 ± 1 °C.

Keywords: Foundry sands, pH test, Self-setting molding sands, Ultrasound

1. Introduction

Quartz sand remains the dominant choice in many foundries, because of its wide availability and low cost, which make it attractive for routine molding sand operations and high-volume casting runs [1]. Quartz sand, which is mainly pure silica (SiO_2), is valued in foundries for its controlled grain distribution and chemical purity, which in turn have a positive effect on obtaining a uniform mold surface and permeability (the ability to remove gases released during liquid metal pouring). Molding sands made with a quartz sand matrix is characterized by very good fluidity. Its thermal properties allow for wide application in industry, not only in foundries but also in glassmaking [2]. Thanks to its neutral pH

(6-7), it can be used for all types of molding sands: green sand, with organic and inorganic binders. Used quartz sand can be reclaimed, in which the binder residues are removed, restoring the shape and surface of the grains to their condition before the molding sand was made (mainly organic binders) [3,4]. This reduces waste and maintains the economic balance of the casting production process. [5,6] Unfortunately, the reclamation process does not restore the chemical properties, which means that acidified sand from molds with an organic system has an acidic reaction, allowing it to be reused only in the same process.

Zircon, corundum, and chromite sands are used for castings that require extreme thermal, chemical, and mechanical properties during production. [7]. Zirconia sand offers thermal stability, and molding sands made from this type of sand has high mechanical strength. It is used in the production of castings as a model sand, where high-quality shape reproduction at elevated temperatures is essential. Unfortunately, due to its high price, it is not widely used in the foundry industry. [8, 9]. Corundum sand, which is dominated by aluminum oxide (Al_2O_3), is also characterized by very good thermal resistance, and molding sands made on the basis of this sand are characterized by low abrasion and long-term dimensional stability at high temperatures. [10, 11]. Chromite sand combines high thermal and mechanical resistance. Molding sands made from this base can also be regenerated. It is used in cast steel foundries as a model sand. [12, 13, 18, 19].

Olivine sand fills the gap between the previously described expensive materials for molding sand cores and quartz sand. Molding sands made of olivine sand are characterized by low thermal expansion, which reduces the occurrence of casting defects associated with thermal stresses. [14, 6].

Molding sands based on quartz sand have been thoroughly researched in terms of hardening kinetics and the production process of molds and cores. [15, 16] This creates a research gap related to the hardening process of molding sands with other foundry sands used as a matrix.

2. Methotology and materials

Based on the method described in standard BN-81/4021-02 [17], the method for determining pH values has been refined. The procedure is as follows:

- The sand sample was dried at 110 °C until a constant mass was obtained.
- After drying, the material was crushed, avoiding grinding the grains.
- Next, 20 g of the prepared sample was weighed.
- The weighed portion of material was transferred to a 100 cm^3 measuring flask.
- Distilled water was added to the flask, filling it to the mark.
- The flask was closed with a stopper and the contents were thoroughly mixed using an ultrasonic cleaner for 15 minutes.
- The flask was then set aside for 24 hours to allow the solution to stabilize.
- After this time, the solution was removed from above the sediment using a pipette (30 ml of filtrate).
- The flask was placed under the pH meter electrode, immersed in the filtrate, and left for at least 3 minutes to allow the measurement to stabilize. [18]

Fourier transform infrared spectroscopy (FTIR) is an analytical technique that uses infrared radiation to study changes in the energy of molecular vibrations and rotations, allowing the identification of functional groups present in a sample [19]. This method enables qualitative analysis of chemical compounds based on characteristic absorption bands or by comparing spectra with reference catalogs [18]. One of the commonly used variants of FTIR is the ATR technique, which allows the examination of samples for which transmission measurements are difficult to perform [20]. The filtrate prepared using the described method was subjected to testing for pH, but in order to better dissolve the compounds responsible for the reaction of the sand, it was left for 72 hours. The tests were carried out using a Nicolet 6700 FTIR spectrometer equipped with an ATR attachment and performing measurements using the SEIRA method, located at the Department of Chemistry and Metal Corrosion of the Faculty of Foundry Engineering at the AGH University of Science and Technology in Krakow. The Origin program was used to process the results of the spectra obtained.

An ultrasonic method was used to analyze the kinetics of molding sand hardening. A sample of the tested sand was placed in a special core box, to which an ultrasonic head was applied to record changes occurring during the setting process over a period of 24 hours. Self-setting molding sands are classified as rheologically unstable materials. These changes in the rheological structure have a significant impact on the propagation of ultrasonic waves during curing. The conditions in the bonding chamber can therefore be considered similar to those in the mold cavity. Based on the analysis of wave velocity, the so-called hardening level (S_x) was determined. The sand hardening level is defined using formula (1), which is based on the dimensionless ultrasonic wave velocity [15, 16, 21, 22]:

$$S_x = \frac{C_{L(x)} - C_{L(0)}}{C_{L(\mathrm{MAX})} - C_{L(0)}} \tag{1}$$

Where:
$C_{L(x)}$ – wave velocity in the sand sample determined in the very moment (t_x),
$C_{L(0)}$ – wave velocity in the sand sample determined at the beginning (t_0),
$C_{L(\mathrm{MAX})}$ – wave velocity in the sand sample after its complete hardening.

Photographs of the bonding brigdes the grains of the sand matrix were taken using a USB microscope MEDIA TECH at 100x magnification.

The Table 1 shows the characteristics of the foundry sands used. In order to prepare the tested molding sands, 1 part by weight of furan resin and 0.5 parts by weight of dedicated hardener per 100 parts by weight of the tested sand were used. The compounds were prepared in a hand mixer, where the matrix was first mixed with the hardener for 30 seconds, and then with the binder for another 30 seconds. In the case of olivine sand, the molding sands were made in the following proportions: 1.0 p.p.w binder /0.5 p.p.w. hardener; 1.0 p.p.w. binder/1.0 p.p.w. hardener; 1.5 p.p.w./1.5 p.p.w. hardener; 1.5 p.p.w./2.5 p.p.w hardener.

Table 1.
Characteristic of foundry sands

	Type of foundry sand						
	Quartz sand	Reclaimed quartz sand	Zirconia sand	Chromite sand	Corundum sand	Olivine sand	Synthetic sand
Main fraction	0.20/0.16/0.32	0.20/0.32/0.40	0.10/0.16/0.20	0.20/0.32/0.40	0.20/0.32/0.16	0.20/0.32/0.40	0.20/0.32/0.40
Main fraction [%]	86.12	93.70	99.10	85.46	98.30	84.88	85.54
Avarage grain size D_L [mm]	0.233	0.287	0.165	0.262	0.243	0.278	0.267
Shape index W_k	1.17	1.46	1.31	1.07	1.59	1.90	1.87
Shape of grain	oval	angular	angular	spherical	sharp - edged	sharp - edged	sharp - edged
Bulk density ρ [g/cm^3]	2.65	2.65	4.60	4.50	3.70	3.30	2.74
Apparent density ρ_0 [g/cm^3]	1.64	1.53	2.83	2.81	1.87	1.71	1.41
Relative density	0.62	0.58	0.62	0.63	0.51	0.52	0.51

3. Results and discussion

3.1. pH test

Figures 1-3 shows a comparison of the results obtained using the method described in standard BN-81/4021-02 with the method developed by the authors, with the median marked. Figure 4 shows the pH measurement values of the tested molding sands.

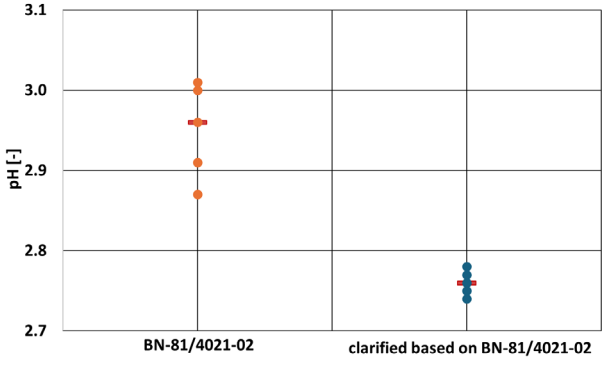

Fig. 1. Comparison of pH testing methods for reclaimed quartz sand

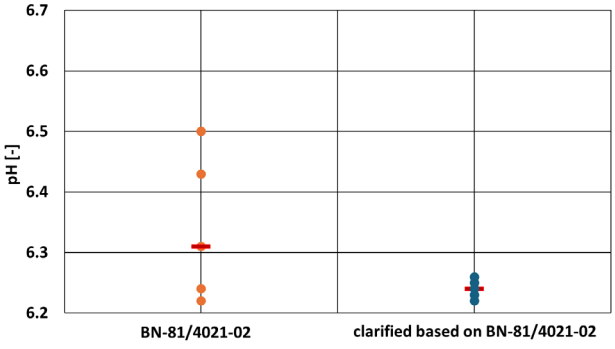

Fig. 2. Comparison of pH testing methods for quartz sand

The method proposed by the authors, based on the method described in standard BN-81/4021-02, shows much greater repeatability of results and greater measurement stability. In each of the results presented, it can be seen that the results in the modified method are close to the median. The results oscillate around one, and the median of the results obtained is also the average result of the measurements. The average deviation from the median for results obtained using the method described in BN81-4021-02 is 0.20, while the modified method proposed in the publication indicates a value of 0.043.

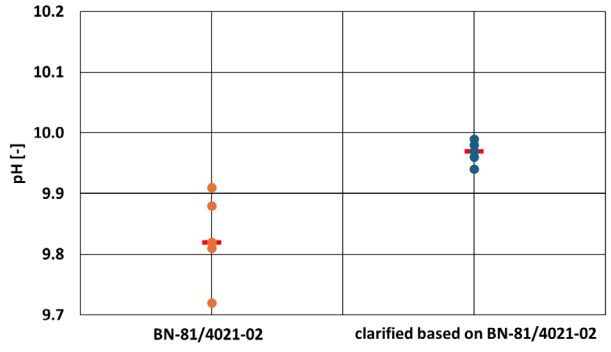

Fig. 3. Comparison of pH testing methods for reclaimed olivine sand

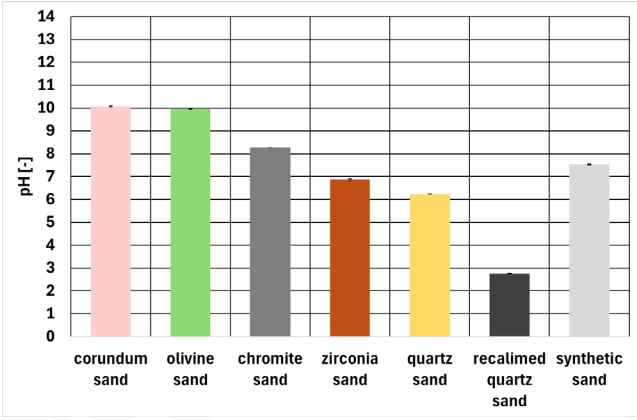

Fig. 4. pH values of the tested molding sands using the method proposed by the authors

The values presented in Figure 4 allow the tested foundry sands to be classified as alkaline, neutral, and acidic. Alkaline sands include corundum sand (pH = 10.08), olivine sand (pH = 9.97), and chromite sand (pH = 8.27). Sands with a neutral chemical character include: zirconia sand (pH = 6.89), quartz sand (pH = 6.24) and synthetic sand (pH = 7.54). The only acidic sand tested is reclaimed quartz sand (pH = 2.76).
The order of magnitude of the standard deviation from the mean is 0.01, which also confirms the repeatability of the results for the modified method by the authors.

3.2. FTIR spectroscopy

On Figure 5 shows the results of FTIR analysis of the tested foundry sands.

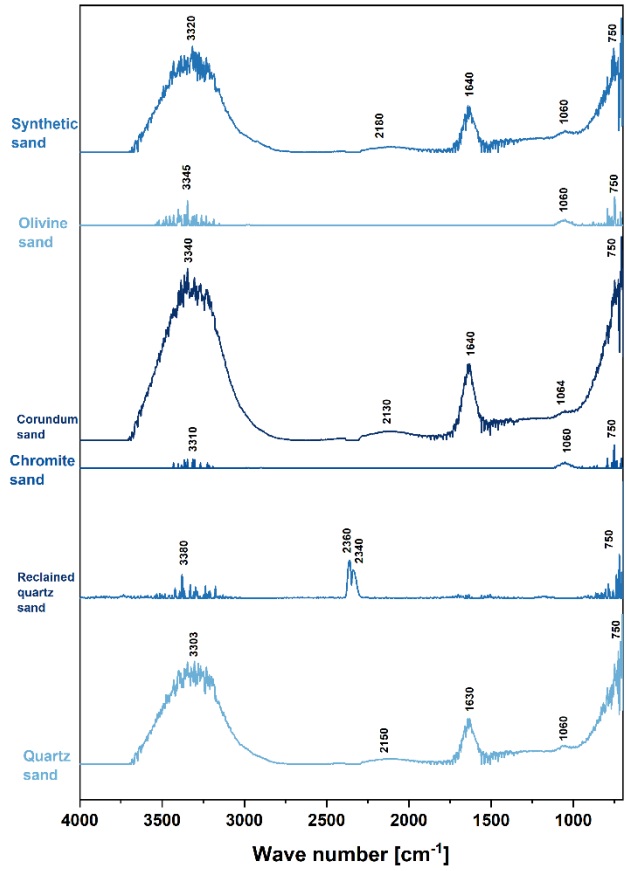

Fig. 5. FTIR analysis of foundry sand samples

The structural analysis of the samples began with the substraction of the background, which was the spectrum of distilled water with a pH of 6. Despite this, due to the dominant absorbance of water, broad peacs characteristic of O-H stretching vibrations are still visible in the obtained FTIR spectra in the range of 3300 – 3350 cm^{-1}. [23] The distinct peaks at 1640 cm^{-1} observed for quartz, corundum and synthetic sand are also typical for water and correspond to the bending vibrations of H-O-H bonds. [24-26] For quartz, chromite, corundum, olivine and synthetic sand, FTIR spectra show peaks or bends characteristic of Si-O groups in the range of 1000-1100 cm^{-1}, more precisely around 1060cm^{-1}. [27] An exception is corundum sand, for which the bend is shifted to 1064 cm-1, which may result from the superposition of bands derived from silicon on other signals, especially those derived from water. However, the presence of this bend clearly indicates the presence of Si-O groups. In the FTIR spectrum of the regenerate, there is no distinct typical band for silicon in the range of 1000-1100 cm^{-1}, but Si-O vibrations can also be seen in the form of bending in the range of 700 – 800 cm^{-1}. [27] These peaks, although varying in intensity, appear in all analysed samples, suggesting that each of the tested sands released silicon compounds into the water. However, it should be emphasized that bands characteristic of metal-O bond vibrations are also observed in the same range, which makes it difficult to unambiguously identify the elements. [28-30] The bands characteristic of aluminum also occur in the 700 – 800 cm^{-1}

range, which overlaps with the range typical for silicon. Therefore, the presence of aluminum in the tested sand samples cannot be unequivocally confirmed. [31] However, the increased intensity of bands in this range for quartz, corundum, and artificial sand may indicate that signals originating from aluminium enhance the absorbance of Si–O groups. In the range of 700 – 800 cm^{-1} in the spectrum of artificial sand, vibrations originating from Ti–O groups are also visible, whose characteristic bands occur in the range of 400 – 700 cm^{-1}, but the release of titanium into water cannot be clearly confirmed [32]. A similar situation applies to olivine, in which the main oxides are magnesium and iron oxides – their characteristic bands also appear in low wave number ranges, which makes it impossible to clearly determine their presence in the solution. In the case of regenerate, the presence of sulphur can be expected. However, the bands characteristic of S=O groups (1100 – 1150 cm^{-1}) may overlap with bands originating from water, which, combined with the small amount of compounds released, makes it impossible to unequivocally confirm the presence of sulphur in the solution. [33] In the analysed FTIR spectrum of the regenerate, peaks derived from S-H groups in the range of 2300 – 2600 cm^{-1} are observed, which may suggest the release of sulphur into water. Based on FTIR spectra of chromite sand, the release of chromium or aluminium cannot be confirmed, as the characteristic bands for these elements occur below 700 cm^{-1}.

The bending in the range of 2000 – 2200 cm^{-1}, visible for quartz sand (2150 cm^{-1}), corundum (2130 cm^{-1}) and artificial sand (2180 cm^{-1}), may be related to the presence of metal-oxygen complexes, but it cannot be ruled out that these are artifacts originating from carbon dioxide, whose bands are observed around 2340 cm^{-1}. [28, 29, 34, 35] These bands are clearly visible in the FTIR spectra of the regenerate. It is worth noting that the FTIR spectra for the regenerate, chromite, and olivine are characterized by very low intensity, which indicates a small amount of compounds released into the solution. As a result, it is difficult to identify specific elements based on these spectra, and the observed signals may result from the overlap of bands originating from different functional groups or from water. The FTIR spectrum of zircon sand showed very low intensity, and after background subtraction no characteristic bands could be identified.

3.3. Kinetics of molding sands hardening

Figures 6–13 present the results of ultrasonic investigations of molding sands prepared on matrices of seven different foundry sands. Due to the strongly alkaline nature of olivine sand, the results obtained for this material were singled out and presented separately in Figures 11–13.

The courses of ultrasonic wave velocity changes during the hardening of the molding sands, depending on the type of sand matrix used, are shown in Figure 6. Regardless of the type of sand matrix employed, two distinct stages can be identified in the recorded binding curves. The first stage is characterized by rapid increases in wave velocity during the binding process, due to the large number of substrates participating in the binding reaction. The second stage is characterized by the wave velocity approaching a constant value, indicating the completion of the binding process.

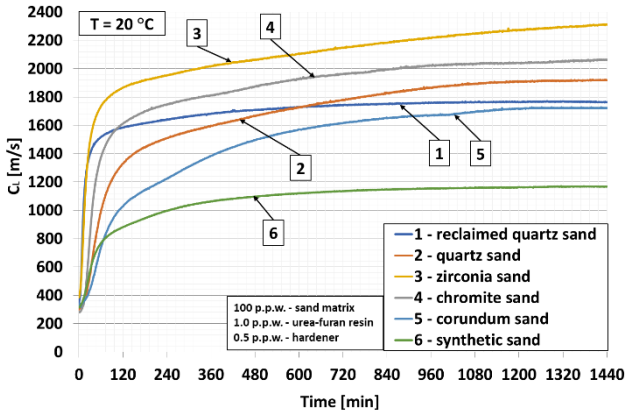

Fig. 6. Influence of the type of sand matrix on the course of ultrasonic wave velocity (C_L) changes during hardening

When analyzing the curves of ultrasonic wave propagation velocity in the binding molding sand, it is important to consider the correlation between the measured wave velocity and the relative density of the sand. The higher the relative density of the molding sand, the higher the wave velocities obtained at the same hardener-to-binder ratio. Another significant aspect is the relationship between wave propagation velocity and the mechanical strength properties of the molding sand. Based on the analysis of the obtained ultrasonic wave velocity curves, it is possible to predict the quality of the formed binder bridges, and consequently, the strength properties of the sand. The higher the final wave velocity achieved during propagation through the molding sand, the better its mechanical performance. Poor quality of the formed binder bridges leads to increased wave attenuation, which is recorded as a decrease in wave velocity [20, 22].

The investigations were carried out using matrices with varying relative densities and different shape index (Table 1). In each case, the molding sand in the specimen was compacted with a piston under a pressure of 60 kPa; therefore, the resulting relative densities of the molding sands were directly determined by the parameters of the matrices themselves (Table 2), rather than by a variable compaction force. The fact that the study was conducted on sand matrices with multiple varying parameters (Table 1) somewhat complicates the analysis of the ultrasonic wave velocity curves in terms of predicting the strength properties of the investigated molding sands. However, it should be noted that the highest wave velocity (Table 2) was obtained for the molding sand prepared on a zircon sand matrix, which had the highest relative density (Table 2) and the smallest mean grain size (Table 1). Conversely, the lowest velocity was observed for the sand prepared on a synthetic sand matrix, which had the lowest relative density (Table 2). These observations confirm the high sensitivity of the ultrasonic method to changes in the relative density of the molding sand, regardless of the type of matrix used. It is likely that the molding sand prepared on the zircon sand matrix exhibited superior mechanical strength properties compared to the sand prepared on the synthetic sand matrix. This is directly related to its relative density as well as to the size and shape of the grains of the matrix itself - smaller grains with a more spherical shape allow the binder to more effectively envelop them and, with appropriate curing of the bonds, form higher-quality binder bridges. Therefore, although the molding

sand based on a corundum sand matrix had a higher bulk density than the sands prepared on reclaimed quartz and quartz sand matrices (Table 2), lower ultrasonic wave velocity values were recorded for it. This is directly related to its low relative density and the shape of the matrix grains. Corundum sand, like synthetic sand, is characterized by angular grains; consequently, the binder cannot fully surround them to form high-quality bridges, which directly results in inferior mechanical properties of the molding sand. The binder bridges formed in the molding sands based on corundum and synthetic sand matrices are localized and do not adhere to the grains as closely as, for example, the bridges in molding sands based on quartz sand (Fig. 14). The poorer quality of intergranular connections in the corundum-based molding sand, combined with its low relative density, causes increased ultrasonic wave attenuation in the molding sand and the recording of lower wave velocity values (Fig. 6, Table 2).

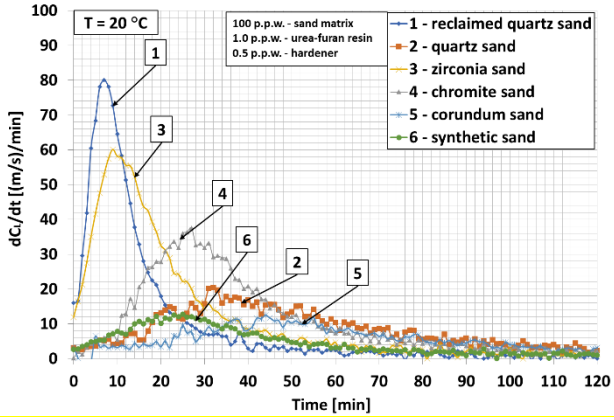

Fig. 7. Influence of the type of sand matrix on the hardening kinetics (dC_L/dt)

The ultrasonic technique constitutes an indirect method that enables the recording of changes in reagent concentration during the hardening process. The kinetics of the molding sand binding process can be determined based on the first derivative of the ultrasonic wave velocity with respect to time (Fig. 7), as well as the first derivative of the degree of hardening with respect to time (Fig. 8). Regardless of the method employed, the obtained curves allow for the analysis of the binding rate of the investigated molding sand and the determination of its working life.

In the ultrasonic method, the bench life of the molding sand is defined as the time elapsed from the moment all components of the molding sand are mixed together until the point at which the maximum rate of the binding reaction is reached [22].

Figures 7 and 8 illustrate the influence of the type of sand matrix on the rate of the molding sand binding process.

The analysis of the obtained results indicates that the highest increase in the hardening reaction rate is observed for the molding sand prepared on a reclaimed quartz sand matrix. This molding sand also exhibits the shortest bench life among the tested samples - approximately 7 minutes (Table 2). The presence of acidic compounds (Fig. 5), resulting from the partial thermal decomposition and oxidation of synthetic resins (carboxylic acids - HCOOH, HC_3COOH) as well as from residual acids from the catalyst that did not react during binding (trace amounts of H_2SO_4) and located on the grain coating of the sand matrix after the regeneration process, serves as an additional source of acidic catalyst, enhancing the effect of the hardener added to the molding sand. The reclaimed quartz sand acts as a surface activator, which, due to the higher concentration of protons originating from sulfonic ($–SO_3H$) and carboxylic (–COOH) groups, creating a stable acidic environment in the reclaimed quartz sand (pH ≈ 2–3, Fig. 4), initiates the resin polycondensation reaction more rapidly. This directly contributes to a more intensive binding reaction and a shortened bench life of the molding sand (Figures 7 and 8) [7].

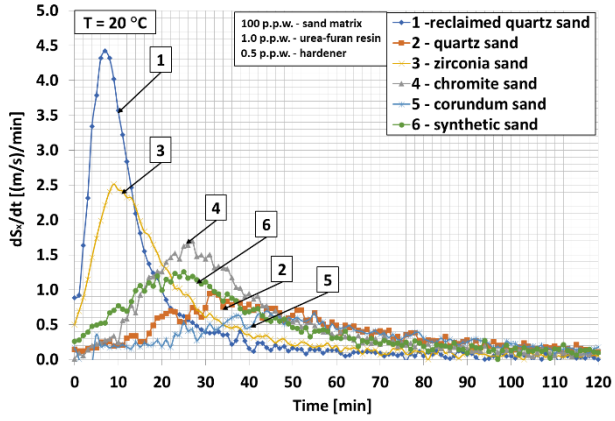

Fig. 8. Influence of the type of sand matrix on the hardening kinetics (dS_x/dt)

The rate of the binding reaction in the molding sand prepared on a zircon sand matrix is lower than that of the molding sand based on reclaimed quartz sand (Fig. 7 and 8). This molding sand also exhibits a slightly longer bench life, approximately 9 minutes (Table 2). The slower hardening rate of the zircon-based sand is attributed to the chemical inertness (Fig. 4) of the zircon grain surfaces ($ZrSiO_4$). Zircon sand possesses a low number of hydroxyl groups (–OH) and a limited capacity to adsorb H^+ ions from the catalyst. The reduced number of protons on the surfaces of zircon grains leads to slower initiation of the resin polycondensation reaction, which proceeds in a more “bulk” rather than surface-oriented manner. The hardening of furfuryl resin occurs via protonation of the furfuryl ring, followed by its opening and the formation of methyl and dimethyl bridges. Weakly acidic surfaces do not facilitate this process. Furthermore, zircon sand has a higher thermal conductivity than reclaimed quartz sand, resulting in a lower local temperature during the exothermic binding reaction, which further slows the hardening kinetics [7].

The binding process of the molding sand prepared on a zircon sand matrix proceeds faster than that of the molding sand based on quartz sand (Fig. 7 and 8) because $ZrSiO_4$ is chemically much more inert than SiO_2. Zircon sand has a more stable crystalline structure with strong Zr–O bonds and significantly fewer reactive surface groups (–OH) than quartz sand, which contains numerous silanol groups (–Si–OH). Consequently, the zircon grains do not neutralize the acidic hardener, which remains fully active and initiates the polycondensation of furfuryl resin more rapidly. Additionally, $ZrSiO_4$ is practically resistant to hydrolysis and exhibits low moisture adsorption, which stabilizes the reaction conditions. Furthermore, zircon sand generally has better grain shape

uniformity, fewer fine fractions and impurities, and a lower specific surface area, meaning it has fewer sites that can potentially react with the catalyst, lower resin demand, and allows for faster and more uniform crosslinking. As a result, the molding sand prepared on a zircon sand matrix hardens more rapidly than sand prepared on the more reactive and surface-active quartz sand [7, 36–39].

The binding process of the molding sand prepared on a chromite sand matrix proceeds more slowly than that of the sand based on zircon sand (Fig. 7 and 8). The bench life of the molding sand is noticeably longer, approximately 27 minutes (Table 2). The primary reason for the slower hardening of chromite-based sand is that this sand ($FeCr_2O_4$) has a more reactive surface than zircon sand ($ZrSiO_4$). As a spinel-type iron and chromium oxide, it contains Fe^{2+}/Fe^{3+} and Cr^{3+} ions within its structure, which provide active ionic centers on the grain surfaces, a higher number of groups capable of reacting with protons, and the potential for surface complexation with anions. As a result, part of the acidic hardener is adsorbed or neutralized on the grain surfaces, reducing the effective concentration of the catalyst in the sand and slowing the resin polycondensation rate. Additionally, chromite sand adsorbs more moisture than zircon sand. The presence of moisture in the molding sand hinders the free progression of resin polycondensation, consequently leading to a further slowdown of the binding reaction [7, 36–39].

Although chromite sand is more reactive than zircon sand, it is less reactive than quartz sand; therefore, the binding process of molding sand prepared on a chromite sand matrix proceeds faster than that of sand based on quartz sand (Figures 7 and 8). The surface of chromite sand grains contains fewer –OH groups than quartz sand grains (–Si–OH) and reacts less with the protons of the hardener. Consequently, more active acidic catalyst remains in the molding sand, and the resin polycondensation reaction proceeds more rapidly. Furthermore, chromite sand adsorbs less moisture than quartz sand, maintaining drier reaction conditions and providing greater stabilization of the process due to reduced acid neutralization by water. In addition, chromite sand has a lower effective specific surface area, which reduces the adsorption of the acidic hardener on the grain surfaces. This results in greater availability of the catalyst and faster resin polycondensation [7, 36–39].

The binding process of the molding sand prepared on a synthetic sand matrix proceeds with lower intensity than that of the molding sand based on chromite sand (Fig. 7 and 8), however, the bench lives of both molding sands are comparable. The bench life of the molding sand prepared on the synthetic sand matrix is approximately 27 minutes (Table 2).

The synthetic sand used is an aluminosilicate produced under controlled conditions. The absence (or significantly lower content) of soluble metal oxides (Fe, Cr, etc.), which are present in chromite sand and can act as local catalytic centers or assist in the hardening of furfuryl resin, results in a milder binding process. Chromite sand contains metal oxides and ions that more readily interact with the reagents (catalysts/resin), which can accelerate polycondensation and lead to a more "vigorous" binding reaction [7, 36–39].

The synthetic sand likely has a more inert surface, resulting in a milder binding reaction. Another factor contributing to the slower hardening of the molding sand on a synthetic sand matrix may be its low content of fine fractions (< 0.09 mm). Fine particles increase the total contact surface and the number of adsorption sites for the acidic catalyst. The manufacturer states that the synthetic sand is designed for use "with all resins" and possesses consistent, predictable properties. This promotes a reproducible and predictable - hence less vigorous - progression of resin polycondensation compared to chromite sand, which exhibits variable characteristics [7, 40].

The molding sand prepared on a synthetic sand matrix hardens faster than the molding sand based on quartz sand (Fig. 7 and 8). Synthetic sand, being an aluminosilicate, likely has a more active grain surface than quartz sand, containing Al–O groups, which enhance the effectiveness of the acidic catalyst. Moreover, the mean grain size of the synthetic sand matrix is slightly larger than that of the quartz sand-based molding sand (Table 1), while the relative density of the molding sand is lower (Table 2). It is likely that the molding sand prepared on the synthetic sand matrix exhibited higher permeability, facilitating vapor exchange from the molding sand to the surroundings, and influencing its binding rate (Fig. 7 and 8) [40].

Table 2.
Characteristic of self-setting molding sands

	Type of molding sand					
	Quartz sand	Reclaimed quartz sand	Zirconia sand	Chromite sand	Corundum sand	Synthetic sand
Apparent density ρ_0 [g/cm^3]	1.61	1.52	2.95	2.77	1.88	1.40
Relative density	0.61	0.57	0.64	0.62	0.51	0.51
$C_{L\,(max)}$ [m/s]	2433.09	2147.13	2777.87	2491.59	2128.49	1333.33
Bench life [min]	32	7	9	27	44	27
S_x = 60 % [min]	338	35	92	118	383	161

The binding process of the molding sand prepared on a quartz sand matrix proceeds gently, with a maximum reaction rate increase of approximately 1 %/min (Fig. 8), while the bench life of the molding sand is around 32 minutes (Table 2). The mild progression of the binding reaction of quartz-based molding sand is determined by the adsorption or partial neutralization of the catalyst by the grain surfaces. Quartz sand grains contain a large number of silanol groups (–Si–OH) (Fig. 5). These groups are capable of adsorbing the acidic hardener, which effectively means that part of the acid is "bound" by the sand surface and does not immediately participate in the resin polycondensation reaction. As a result, the initial binding rate is somewhat slower than it would be if the acid remained fully active. Zircon, chromite, synthetic, or reclaimed quartz sands contain fewer active surface groups capable of adsorbing the acid. In these sands, the acid within the catalyst remains fully active, leading to a faster initiation of resin polycondensation and a shorter hardening time under similar temperature conditions and at the same binder and catalyst content (Fig. 7 and 8) [7, 36–39].

The last molding sand examined, for which the binding process results are presented in Figures 7 and 8, is the molding sand prepared on a corundum sand matrix. The binding process of the corundum-based molding sand exhibits the mildest course, with a maximum reaction rate increase of 0.7 %/min (Fig. 8). The bench life of the molding sand is the longest among the samples studied, approximately 44 minutes (Table 2). Corundum sand is composed of aluminum oxide (Al_2O_3) with a very stable and dense crystalline lattice. The surface of corundum sand grains is practically chemically inert. Unlike quartz sand, it does not possess –Si–OH groups that could partially adsorb the acid present in the catalyst, and it also lacks transition metal ions (such as Fe^{2+} in chromite sand) that could accelerate the reaction. As a result, the absence of surface interactions means that the resin polycondensation reaction is initiated solely by the dissolved catalyst and resin molecules, without any "accelerating stimuli." The very low surface activity of corundum sand causes the catalyst to remain "immobile" on the surface, while also not being locally concentrated in any way. Consequently, the resin polycondensation reaction proceeds uniformly, slowly, and gently, without sudden "bursts." Furthermore, corundum sand is highly thermally stable and insulating, so the exothermic resin polycondensation process is neither enhanced nor locally accelerated. Additionally, the angular shape of the matrix grains hinders the uniform distribution of both the hardener and the binder across the grain surfaces. As a result, the molding sand with organic binder prepared on a corundum sand matrix hardens the slowest, and the binding process itself exhibits the mildest course (Fig. 7 and 8) [7, 36–39].

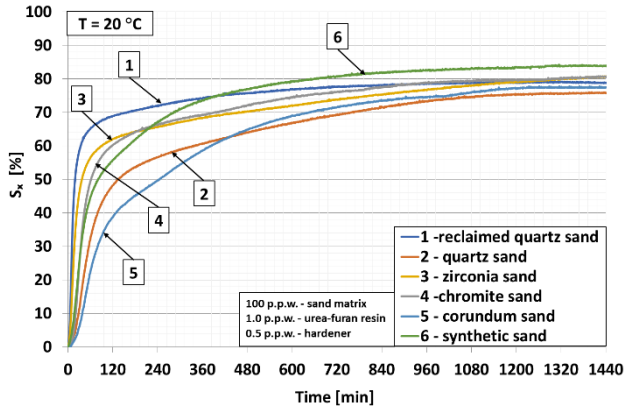

Fig. 9. Influence of the type of sand matrix on the course of changes in the degree of hardening (S_x) during the bonding process

Figure 9 illustrates the influence of the type of sand matrix on the progression of the degree of hardening of molding sand with an organic binder. Based on the obtained curves of the hardening degree, it is possible to determine key parameters of the molding sand, such as the initial hardening time, after which the model can be safely removed from the mold without risk of damage (S_x = 60–70 %), and the time for complete hardening, after which the mold can be safely poured with molten metal (S_x should be at least 90 %) [20, 22].

Table 2 presents the initial hardening times (S_x = 60 %) of molding sands with an organic binder, depending on the type of sand matrix used. The shortest initial hardening time was recorded for the molding sand prepared on a reclaimed quartz sand matrix - approximately 35 minutes - while the longest was observed for the molding sand based on a corundum sand matrix, approximately 383 minutes. For the molding sand prepared on a quartz sand matrix, the initial hardening time was about 338 minutes.

After 24 hours of monitoring the hardening process, the investigated molding sands reached a degree of hardening ranging from 76 % for the molding sand based on quartz sand to approximately 84 % for the molding sand prepared on a synthetic sand matrix. These levels of hardening are not sufficient to allow mold pouring with molten metal. However, when interpreting these results, it should be taken into account that the experiments were conducted in a test specimen, where the conditions throughout the measurement corresponded to those directly adjacent to the model, limiting vapor exchange from the molding sand to the surroundings. After 24 hours of monitoring the binding process, a continuous increase in the degree of hardening was observed, indicating that the binding process was still ongoing (Fig. 9). Under industrial conditions, the mold would be disassembled to remove the model, facilitating the removal of vapors from the central parts of the mold. Consequently, molds prepared with the investigated molding sands (Fig. 9) could be safely poured with molten metal 24 hours after preparation.

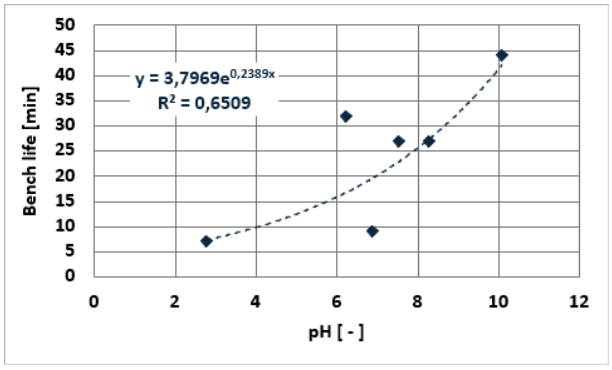

Fig. 10. Influence of the sand matrix pH on the bench life of self-setting molding sands with an organic binder (σ_y = 12.88; σ_e = 7.61)

Based on the conducted studies, the influence of the pH of the sand matrix on the working life of self-setting molding sands with an organic binder was determined. Analysis of the data presented in Figure 10 indicates a general trend of increasing molding sand bench life with rising pH of the applied matrix. However, a detailed consideration of this relationship requires taking into account the compositions of the sand matrices themselves (Table 3), which determine the resulting pH value and the behavior of individual compounds with respect to the acidic hardener (Table 4). Equally important are the size and shape of the individual matrix grains, which affect the ability to uniformly distribute the acidic hardener and resin across the surfaces, as well as the presence of fine fractions and various types of impurities. For this reason, the bench life of the molding sand prepared on a zircon sand matrix, despite a pH of 6.89, was only 9 minutes, whereas for the molding sand based on quartz sand (pH = 6.24) it was 32 minutes. Zircon sand contains compounds that have a neutral effect on the resulting pH while exhibiting no activity toward the acidic hardener (Tables 3 and 4), and the grain size of the matrix is relatively small (Table 1). In contrast, quartz sand contains CaO, K_2O and Na_2O, which neutralizes the effect of the acidic catalyst (Tables 3 and 4). The presence of basic compounds, combined with the larger grain size of the quartz sand matrix (Table 1), as well as the presence of silanol groups on the grain surfaces, which are capable of adsorbing the acidic hardener, results in an extended binding time and an increase in the bench life of the molding sand.

It should be noted, however, that the pH index reflects only the content of water-soluble acidic and basic substances. Foundry sands also contain water-insoluble acid–base compounds, such as magnesium carbonate ($MgCO_3$) or calcium carbonate ($CaCO_3$), which reacts with the acidic catalyst to form calcium salts, CO, and water. Therefore, relying solely on the pH index when attempting to assess the bench life of a molding sand may lead to certain inaccuracies, as illustrated in Figure 10. A more precise analysis should employ the Acid Demand Value (ADV), which accounts for the presence of impurities in the examined sand that are insoluble in water yet react with the acidic catalyst [41].

Table 3.
Sample composition of foundry sands [7, 40, 42-45]

		Type of foundry sand					
		Quartz sand	Zirconia sand	Chromite sand	Corundum sand	Olivine sand	Synthetic sand
Content [%]	**SiO_2**	97.60	31.60-32.60	0.25-1.00	0.03-0.15	41.70	52.10-55.60
	ZrO_2+HfO_2		63.06-65.5				
	Cr_2O_3			min. 46.00		0.31	
	Al_2O_3	1.00	0.70-3.00	15.00-16.00	99.00	0.46	min. 41.00
	MgO			9.00-11.00		49.60	
	Fe_2O_3	0.15	0.05-0.11	25.00-29.50	0.02-0.08	7.40	max. 1.50
	$CaCO_3$	0.20					
	K_2O	0.50					
	TiO_2		0.26-0.85				1.40-1.70
	NiO					0.32	
	MnO					0.09	
	CaO	0.20		max. 0.15			
	Na_2O	0.25			0.10-0.30		

Table 4.
pH in water of oxides/carbonates present in foundry sands and their reaction in the presence of an acidic hardener [36-39]

Oxide / Carbonate	Solubility / Reaction in water	pH in water	Effect on pH in water	Chemical character	Behavior with acidic hardener
SiO_2	very slightly soluble, does not react in normal water	practically neutral, chemically acidic oxide	no significant effect/ lightly acidic	acidic	minimal effect on curing; possible partial adsorption
ZrO_2+HfO_2	insoluble in water	neutral	no effect	amphoteric	insoluble; no effect on polycondensation
Cr_2O_3	insoluble in water, amphoteric (reacts only with acids or strong bases)	practically neutral	no effect	amphoteric	practically insoluble; negligible effect
Al_2O_3	insoluble in water, amphoteric	practically neutral	no effect	amphoteric	insoluble; minimal effect
MgO	reacts with water forming $Mg(OH)_2$	slightly basic	increases pH	basic	neutralizes some acid → slows curing
Fe_2O_3	insoluble in water	neutral	minimal effect	amphoteric	no significant effect; possible partial adsorption
$CaCO_3$	practically insoluble in water; no reaction with pure water, slightly soluble in the presence of CO_2 forming $Ca(HCO_3)_2$	slightly basic (pH of the aqueous suspension)	slightly increases pH	basic (salt of a weak acid and a strong base)	reacts with acids with CO evolution, forming soluble calcium salts and H_2O
K_2O	reacts with water forming KOH	strongly basic	increases pH	basic	neutralizes acid → slows curing
TiO_2	insoluble in water	neutral	no significant effect	amphoteric	minimal effect
NiO	practically insoluble in water at room temperature, it can react slightly with water to form $Ni(OH)_2$	slightly basic	slight increase	basic	neutralizes acid → slows curing
MnO	practically insoluble in water at room temperature, it can react slightly with water to form $Mn(OH)_2$	slightly basic	increases pH	basic	neutralizes acid → slows curing
CaO	reacts with water forming $Ca(OH)_2$	strongly basic	increases pH	basic	neutralizes acid → slows curing
Na_2O	reacts with water forming NaOH	strongly basic	increases pH	basic	neutralizes acid → significantly slows curing

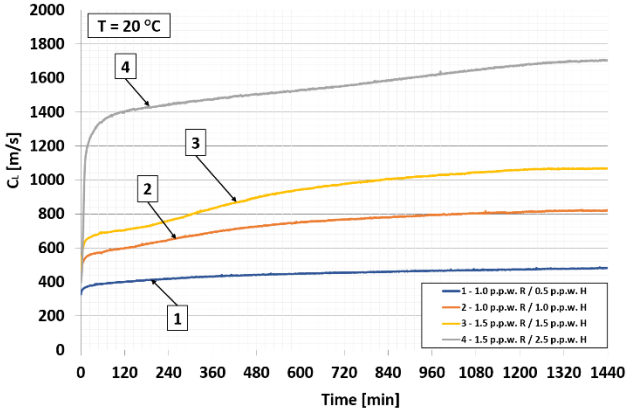

Fig. 11. Effect of the hardener-to-resin ratio (H/R) on the course of ultrasonic wave velocity (C_L) changes in the olivine-based molding sand

Figures 11–13 present the results of tests performed on organically bonded self-setting molding sands prepared using an olivine sand matrix, with varying hardener-to-resin ratios. Olivine sand ($(Mg,Fe)_2SiO_4$) is considered incompatible with self-setting systems based on organic binders, particularly when standard hardener proportions are used. This is due to the presence of alkaline-earth metal ions (Mg^{2+}, Fe^{2+}) (Fig. 5), which adsorb the acidic catalyst, resulting in partial or complete neutralization of the hardener. Consequently, the initiation of resin polycondensation is significantly slowed or even prevented at standard hardener levels. For research purposes, however, it was decided to determine the hardener and resin contents at which the curing process of the olivine-based molding sand could be successfully recorded [7, 36–39].

Olivine sands often contain a high proportion of fine particles (< 0.1 mm) and dust, which adsorb the acidic catalyst and reduce its effective availability within the molding sand. Moreover, olivine sand typically exhibits an irregular, angular grain morphology and

a relatively high relative density in the loose state (Table 1). These factors may impede the diffusion of the acidic hardener throughout the molding sand and lead to non-uniform curing, which is particularly disadvantageous when standard hardener-to-resin ratios are applied [7].

Figure 11 illustrates the effect of the hardener-to-resin ratio on the course of ultrasonic wave velocity changes in the molding sand prepared on an olivine sand matrix. As the content of both the hardener and the resin increases, progressively higher wave propagation velocities are recorded. This indicates that the molding sand develops increasingly better strength properties. However, the molding sands labelled 1-3 (Fig. 11) do not exhibit the characteristic ultrasonic velocity profile typically observed during curing - namely, an initial stage with intensive increases in wave velocity followed by a second stage in which the curing process stabilizes. An insufficient amount of hardener in the molding sand was unable to "overcome" the neutralizing effect of the olivine sand grain surfaces. Consequently, these molding sands did not cure, and during the attempt to remove the specimen from the tester, they disintegrated. The only olivine-based molding sand for which a characteristic ultrasonic wave velocity profile could be recorded was mixture number 4 (Fig. 11), containing 2.5 p.p.w. of hardener and 1.5 p.p.w. of resin. Unlike the remaining molding sand, this one did not undergo destruction upon removal from the test specimen holder. It should be noted, however, that despite the increased content of both hardener and resin - where the latter would normally enhance the mechanical performance of the molding sand - the recorded ultrasonic wave velocity remained relatively low. This likely indicates that the molding sand developed only modest strength, which additionally may be attributed to its high porosity (low relative density).

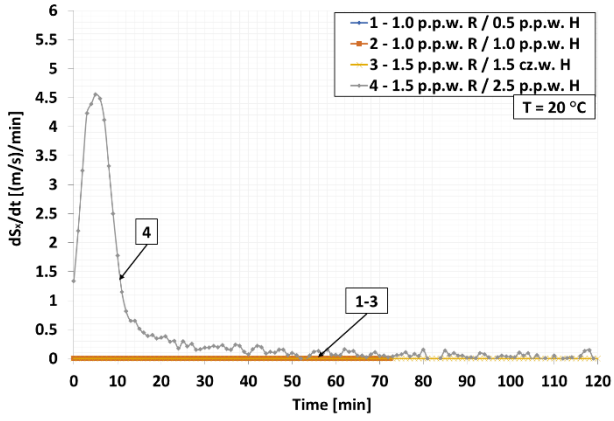

Fig. 12. Effect of the H/R ratio on the hardening kinetics (dS_x/dt) of the olivine-based molding sand

A molding sand based on olivine, even when it eventually cures, will be weaker and more brittle than, for example, a quartz-sand-based molding sand cured under standard proportions. Excess acid disturbs the resin's crosslinking structure, leading to regions that are either insufficiently crosslinked or excessively crosslinked. Moreover, an overabundance of acidic hardener may also induce partial acid-catalyzed degradation of the resin.

Figure 12 presents the effect of the hardener-to-resin ratio on the curing kinetics of the molding sand prepared on an olivine sand matrix. The hardening process of mixture number 4 is exceptionally intense, with a maximum reaction rate of approximately 4.5 %/min and a bench life of only about 6 minutes. This behavior results from exceeding the threshold of neutralization of the acidic hardener. Neutralization continues only until the olivine sand grain surfaces become "saturated" with acid. Beyond this point, the initially mild reaction transforms into a very rapid and highly exothermic process. As a consequence, the molding sand undergoes extremely fast, difficult-to-control hardening, leading to localized zones of intensive resin polycondensation and an increased risk of overheating. These phenomena can result in heterogeneous mechanical properties of the cured molding sand. Furthermore, increasing the dose of the acidic hardener drastically shortens the bench life of the molding sand, potentially preventing the successful production of complex molds or cores.

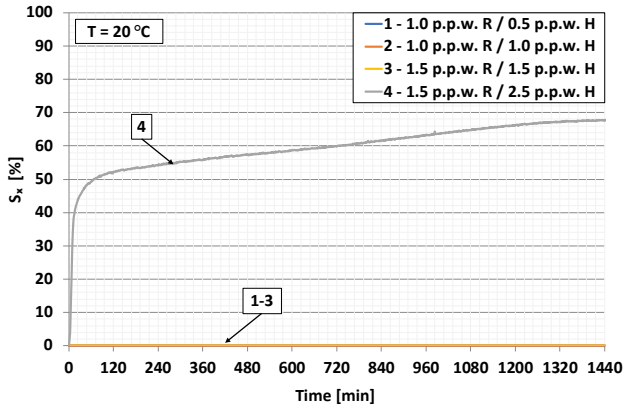

Fig. 13. Effect of the H/R ratio on the course of changes in the degree of hardening (S_x) of the olivine-based molding sand

The initial hardening time of molding sand number 4 prepared on an olivine sand matrix (Fig. 13) is approximately 720 minutes, and after 24 hours of monitoring the hardening process, the molding sand reaches a degree of hardening of about 68 %.
It should be noted, however, that the experiments conducted on the olivine-based molding sand had only an exploratory character. An excess of acidic hardener in the molding sand causes a range of foundry-related issues gas evolution increases, the risk of burns, sintering, and excessive resin consumption rises, which in turn leads to a higher content of resin degradation products that deteriorate casting quality. Consequently, olivine sand is considered incompatible with systems based on organic binders, and "rescuing" the molding sand by increasing the acidic hardener content results in destabilization of the entire system [7].

3.4. Observation of bonding bridges

Figure 14 shows microscopic images of the tested molding compounds.

Fig. 14. Microscopic analysis of bonding bridges

Quartz sand and reclaimed quartz sand molding compounds indicate the highest number of binding bridges between the matrix grains, referring to the data presented in Table 1. The shape of the grains is oval, which will have a positive effect on the strength properties of the tested molding compounds. The bridges shown for quartz sand and reclaimed quartz sand are associated with good surrounding by the matrix grain binding system.

Chromite sand, it can be seen that the shape of the grains (spherical) defines the nature of the connecting bridges, which is more point-like than surface-like. The grains of the matrix are usually connected in one place.

In the case of zircon sand, the most distinct bridges between the matrix grains can be observed. The binder used forms extensive bonding bridges, which can have a positive effect on the strength properties of molding compounds and good surface quality. However, when pouring liquid metal into the mold, this can cause higher local gas generation, which can contribute to the formation of gas-related defects.

The molding sand made on a corundum sand matrix is characterized by sharp-edged grains, and the binding bridges are point-like, similar to the molding sand made on a chromite sand matrix.

An analysis of the binder bridges in the olivine sand-based molding sand shows that the matrix grains are well surrounded by the binder material (due to the increased amount of binder in the molding sand) and that there are surface binder bridges, which may have a positive effect on the properties of the tested sand.

The molding sand made on the basis of artificial sand exhibits the properties of binding bridges as in the case of sands made on a quartz matrix. The binding bridges are surface-based and clearly marked.

4. Conclusions

Based on the research, the following conclusions were drawn:

1. The modified method for determining the pH value of the sand matrix proposed by the authors, based on the BN-81/4021-02 standard, is characterized by high repeatability of the obtained results and excellent measurement stability - the order of magnitude of the standard deviation from the median is, on average, 0.01.
2. Among the key factors influencing the course of the binding process in self-setting molding sands with an organic binder are: the type and amount of binder and hardener used, the temperature of the individual molding sand components and the surrounding environment, the type of sand matrix applied, as well as the size and shape of the sand matrix grains.
3. The surface activity of sand matrix grains in relation to the acidic hardener is one of the factors determining the progress of the molding sand binding process.
4. Acidic compounds present on the grain surfaces of the matrix after the reclamation process constitute an additional source of acidic catalyst, enhancing the effect of the hardener introduced into the molding sand. The reclaimed quartz sand acts as a surface activator, initiating a more rapid progression of the resin polycondensation process, which consequently leads to a reduction in the bench life of the molding sand.
5. The bonding process of molding sands prepared on a matrix whose grain surfaces are chemically inert, characterized by an approximately spherical grain shape and fine grain size, proceeds more rapidly and with greater intensity than in the case of molding sands based on a matrix that partially adsorb or neutralize the action of the acidic hardener and are composed of large, angular grains.
6. With increasing pH of the sand matrix, a general trend of extending the bench life of the molding sand is observed. However, when analyzing this relationship in detail, it is necessary to consider the chemical composition of the sand matrices themselves, which determines the measured pH value, as well as the behavior of individual compounds in the presence of the acidic hardener - their surface activity and the

presence of dust fractions or various impurities (e.g., carbonates).

Further research will include a detailed analysis of the chemical composition (ICP), strength tests of the proposed molding compounds, as well as a more detailed observation of the bonding bridges (SEM/EDS). In addition, tests related to the use of an inorganic bonding system are planned.

Acknowledgements

Special thanks to prof. U. Lelek-Borkowska and W. Oksiutowicz their assistance in conducting the tests: pH measurement and FTIR tests, and to prof. J. Zych for providing the measuring equipment for the kinetics of hardening molding sand tests.

The research was co-financed by AGH Research Project No 501.00 170000 10000.

References

[1] Radkovský, F., Gawronová, M., Merta, V., Lichý, P., Kroupová, I., Nguyenová, I., Kielar, Š., Folta, M., Bradáč, J. & Kocich, R. (2022). Effect of the composition of hybrid sands on the change in thermal expansion. *Materials.* 15(17), 6180, 1-15. DOI: 10.3390/ma15176180.

[2] Svidró, J., Svidró, J.T. & Diószegi, A. (2020) The role of purity level in foundry silica sand on its thermal properties. *Journal of Physics: Conference Series.* 1527, 012039, 1-7. DOI: 10.1088/1742-6596/1527/1/012039.

[3] Kabasele, J.K. & Nyembwe, K.D. (2025) An assessment of south african chromite sand crushing ratio. *International Journal of Metalcasting.* 19(2), 619-634. DOI: 10.1007/s40962-024-01337-1.

[4] Sabour, M.R., Akbari, M. & Dezvareh, G. (2020) Utilization of color change and image processing to evaluate the Waste Foundry Sand reclamation level. *Journal of Materials Research and Technology.* 9(1), 1025-1031. DOI: 10.1016/j.jmrt.2019.11.041.

[5] Łucarz, M., Garbacz-Klempka, A., Brzeziński, M., Pribulová, A. & Fedorko, P. (2024). Investigation of spent moulding sand using thermal treatment with regard to the possibility of recovering quartz matrix. *Materials.* 17(23), 5991, 1-26. DOI: 10.3390/ma17235991.

[6] Yu, Y., Yang, M., Wan, C. & Lang, L. (2025). Mechanical, workability, economic and environmental properties of concrete with limestone calcined clay cement and recycled aggregates. *Scientific Reports.* 15(1), 14122, 1-15. DOI:10.1038/s41598-025-97539-6.

[7] Lewandowski, J.L. (1997). *Materials for casting moulds*. Kraków: Akapit. (in Polish)

[8] Wiśniewska, K., Madej, D. & Szczerba, J. (2018). The corrosion of Mg-partially stabilized zirconiaduring service in continuous casting tundish. *Journal of Ceramic Science and Technology.* 09(3) 301-308. DOI: 10.4416/JCST2018-00019.

[9] Liu, L., Shan, Z., Liu, F. & Dun, L. (2018). High-quality manufacturing method of complicated castings based on multi-material hybrid moulding process. *China Foundry.* 15(5), 343-350. DOI: 10.1007/s41230-018-8053-y.

[10] Storozhenko, P.A., Shcherbakova, G.I., Sidorov, D.V., Varfolomeev, M.S. & Murkina, A.S. (2010). Corundum molds for investment casting from refractory alloys and metals. *Advances in Materials Science and Engineering.* 2010, 954507, 1-5. DOI: 10.1155/2010/954507.

[11] Holtzer, M., Bobrowski, A., Drożyński, D. & Mocek, J. (2013). Selection of protective coatings of moulds for castings of high-manganese cast steel in dependence of the applied moulding sand kind. *Archives of Metallurgy and Materials.* 58(3), 853-857. DOI: 10.2478/AMM-2013-0086.

[12] Kabasele, J.K., Nyembwe, K.D. & Polzin, H. (2023). Assessment of foundry chromite sand crushability under thermal-mechanical loading. *Archives of Foundry Engineering.* 23(3), 16-21. DOI: 10.24425/afe.2023.144310.

[13] Kabasele, J. & Nyembwe, D. (2021). Assessment of local chromite sand as 'green' refractory raw materials for sand casting applications in a post-pandemic world. *South African Journal of Industrial Engineering.* 32(3), 65-74. DOI: 10.7166/32-3-2615.

[14] Stachowicz, M., Pałyga, Ł. & Kępowicz, D. (2020) Influence of automatic core shooting parameters in hot-box technology on the strength of sodium silicate olivine moulding sands. *Archives of Foundry Engineering.* 20(1), 67-72. DOI: 10.24425/afe.2020.131285.

[15] Matonis, N. & Zych, J. (2023). Kinetics of binding process of furan moulding sands, under conditions of forced air flow, monitored by the ultrasonic technique. *Archives of Foundry Engineering*. 23(4), 93-98. DOI: 10.24425/afe.2023.146683.

[16] Matonis, N. & Zych, J. (2022). Plasticity changes of moulding sands with chemical binders caused by increasing the hardening degree. *Archives of Foundry Engineering.* 22(2), 71-76. DOI: 10.24425/afe.2022.140227.

[17] BN-81/4021-02 - *Odlewnicze materiały formierskie - Piaski kwarcowe regenerowane (Foundry molding materials - Regenerated quartz sands)*. Wydawnictwa Normalizacyjne (Standardization Publications): Warsaw, Poland, 1982. (in Polish).

[18] Kamińska-Bach, G. (2008). Infrared spectroscopy in the analysis of polymer materials: characteristics of the method and various areas of application. *Przetwórstwo Tworzyw.* 14(3), 70-74. (in Polish).

[19] Kazarian, S.G. & Chan, K.L.A. (2013). ATR-FTIR spectroscopic imaging: recent advances and applications to biological systems. *Analyst.* 138(7) 1940-1951. DOI: 10.1039/c3an36865c.

[20] Matonis N. (2025). *Application of ultrasonic technique for studying the kinetics of binding processes of self-setting moulding sands.* Doctoral Thesis, Kraków, AGH University of Krakow.

[21] Zych J. (1999) Patent Nr PL 192202 B1. Kraków

[22] Zych, J. (2007). *Synthesis of the applications of ultrasonic technology in the analysis of the kinetics of selected processes occurring in molding materials*. AGH Uczelniane Wydawnictwa Naukowo-Dydaktyczne. Seria: Rozprawy i Monografie nr 163, Kraków. (in Polish)

[23] Yeming, X., Pai, L. & Yunhong, Z. (2022) Mid-infrared spectroscopy of hemispherical water droplets. *Spectrochemia*

Acta Part A: Molecular and Biomecular Spectroscopy. 264, 120256. DOI: 10.1016/j.saa.2021.120256.
[24] Seaman S.J., Dyar, M.D., Marinkovic, N. & Dunbar, W. (2006). An FTIR study of hydrogen in anorthoclase and associated melt inclusions. *American Mineralogist.* 91(1) 12-20. DOI: 10.2138/am.2006.1765.
[25] Risakotta, M.Y.S. & Andayany, H. (2020). Mineral identification of rocks from Pohon Batu hot springs in West Seram using FTIR spectroscopy. *Journal of Physics: Conference Series.* 1572, 012045, 1-6. DOI: 10.1088/1742-6596/1572/1/012045.
[26] Szymańska-Pulikowska, A., Wdowczyk, A. & Wiercik, P. (2023) Analysis of changes on substrates filling constructed wetland systems after landfill leachate treatment - FTIR study. *Journal of Cleaner Production.* 411, 137336, 1-11. DOI: 10.1016/j.jclepro.2023.137336.
[27] Sazali, R., Sorbie, K., Boak L., Azman, A. Z., Saaid, I. M., Dollah, A., Kassim Shaari, N.Z.B. & Ismail, K. (2023). The characterization study of inhibited silica/silicate scale using vinyl sulfonated copolymer (VS-Co). Journal of *Achievements in Materials and Manufacturing Engineering*. 117(2), 57-70. DOI: 10.5604/01.3001.0053.6699.
[28] Yuspova, A., Rezida, A., Baraeva, L. & Shafigullin, L. (2021). Investigation of the activating effect of metal chlorides (Al, Zn, Ti, Fe) in the reactions of surface functional groups of amorphous silicon dioxide. *Materialstoday: Proceedings.* 38(4), 1653-1658. DOI: 10.1016/j.matpr.2020.08.177.
[29] Mogorosi, R.P., Fischer, N., Claeys, M. & van Steen, E. (2012). Strong-metal–support interaction by molecular design: Fe–silicate interactions in Fischer–Tropsch catalysts. *Jorunal of Catalysis.* 289, 140-150. DOI: 10.1016/j.jcat.2012.02.002.
[30] Wiergowski, M., Sołtyszewski, I. & Sein Amand, J. (2015). Chemical analysis of wastewater as a new way of monitoring drugs and medicines consumption at workplace. *Medycyna Pracy.* 66(6), 837-847. DOI: 10.13075/mp.5893.00188 (in Polish).
[31] Kumar, K., Rajasekhar, K. & Sashidhar, C. (2024). Evaluation of durability and microstructural properties of waste foundry sand as a sustainable alternative to M-sand in concrete production. *SSRG International Journal of Civil Engineering.* 11(5), 11-21. DOI: 10.14445/23488352/IJCE-V11I5P102.
[32] Pires, C.T.G.V.M.T, Oliveira, Jr N.G. & Airoldi, C. (2012). Structural incorporation of titanium and/or aluminum in layered silicate magadiite through direct syntheses. *Materials Chemistry and Physics.* 135(2-3), 870-879. DOI: 10.1016/j.matchemphys.2012.05.072.
[33] Yusuf, M.O. (2023). Bond characterization in cementitious material binders using fourier-transform infrared spectroscopy. *Applied Sciences.* 13(5), 3353, 1-27. DOI: 10.3390/app13053353.
[34] Maciejewska, A. (2015). Influence of spectral interferences on the results of quartz determination by infrared spectrometry. *Workers' health and safety.* 66(4), 497-509. DOI: 10.13075/mp.5893.00212. (in Polish).
[35] Petrova, T.M., Solodov, A.M., Solodov, A.A., Lyulin, O.M., Borkov, Yu.G., Tashkun, S.A. & Perevalov, V.I. (2015). Measurements of CO2 line parameters in the 9250–9500 cm^{-1} and 10,700–10,860 cm^{-1} regions. *Journal of Quantitative Spectroscopy and Radiative Transfer.* 164, 109-116. DOI: 10.1016/j.jqsrt.2015.06.001.
[36] Eds. Ertl G., Knözinger, H., Schüth, F., Weitkamp, J. (2008). *Handbook of Heterogeneous Catalysis* 2. Weinheim: Wiley-VCH.
[37] Adamson, A., Gast, A. (1997). *Physical Chemistry of Surfaces*. New York: John Wiley & Sons.
[38] Rao, C.N.R. (1974). *Chemistry of the Solid State*. New York: M. Dekker.
[39] Holtzer, M., Staronka, A. (2000). *Physical chemistry*. Kraków: AGH Uczelniane Wydawnictwa Naukowo-Dydaktyczne (in Polish).
[40] Sand Team. (2015, June). *Technický list - LK-SAND.* Retrieved December 8, 2025, from https://www.sandteam.cz/new/wp-content/uploads/2015/05/LK_SAND.pdf. (in Czech).
[41] Dańko, J., Holtzer, M., Kargulewicz, I., Lewandowski, J.L., Zapalski, A. (1998). Possibility of using the method of determining the acid demand (Zk) to assess the quality of the regenerated mass from cement. *Acta Metallurgica Slovaca*. 4(2), 136-140. (in Polish).
[42] Sand Team (2015, June). *Technický list - OLIVÍN*. Retrieved December 8, 2025, from https://www.sandteam.cz/ new/wp-content/uploads/2015/05//Olivín.pdf (in Czech)
[43] Sand Team. (2015, June). *Technický list - CHROMITOVÝ PÍSEK.* Retrieved December 8, 2025, from https://www.sandteam.cz/new/wp-content/uploads/2015/05/Chromit.pdf (in Czech)
[44] KRATOS Polska. (2014, March). *Product Information Sheet - Zirconium Sand CR 023*. Retrieved December 8, 2025, from https://kratos.pl/wp-content/uploads/2018/02/ Karta-informacyjna-piasek-cyrkonu-CR023.pdf. (in Polish).
[45] SIBELCO POLAND. (2018, August). *Product technical data sheet – BK 50D*. Unpublished materials from the sales representative) (in Polish).